Rovibrational Energy Transfer in the $4\nu_{CH}$ Manifold of Acetylene, Viewed by IR−UV Double Resonance Spectroscopy. 1. Foundation Studies at Low J†

Mark A. Payne, Angela P. Milce, Michael J. Frost,‡ and Brian J. Orr*

Centre for Lasers and Applications, Macquarie University, Sydney, NSW 2109, Australia

Received: May 6, 2003; In Final Form: August 15, 2003

Time-resolved infrared-ultraviolet double resonance (IR−UV DR) spectroscopy is used to prepare acetylene molecules (C_2H_2) in specific rovibrational states of the 12 700 cm^{-1} $4\nu_{CH}$ manifold of the electronic ground-state $\tilde{X}$, monitoring their direct excitation and collision-induced state-to-state energy transfer, by probing at ∼299 or ∼296 nm with laser-induced fluorescence via the $\tilde{A}$ electronic state. The $4\nu_{CH}$ manifold derives much of its IR brightness from the ($\nu_1 + 3\nu_3$) combination band, such that many of the rotational levels J monitored by IR−UV DR are derived from the $(1\ 0\ 3\ 0\ 0)^0$ vibrational state. The $4\nu_{CH}$ manifold of C_2H_2 is congested and affected by anharmonic, l-resonance, and Coriolis couplings that cause other IR-dark, UV-bright rovibrational levels to attain appreciable IR−UV DR intensity and to add to the complexity of intramolecular dynamics in that manifold. Consequently, collision-induced rovibrational satellites observed by IR−UV DR comprise not only regular even-ΔJ features but also supposedly forbidden odd-ΔJ features, of which the energy-transfer channel from $J = 12$ to $J = 1$ is particularly efficient. This paper focuses on low-J rovibrational levels of the $4\nu_{CH}$ manifold, particularly those with $J = 0$ and $J = 1$ in view of their anomalously large Stark effects that are likely to make them susceptible to collision-induced rovibrational mixing. Three complementary forms of IR−UV DR experiment are reported: IR-scanned, UV-scanned, and kinetic. These indicate that strong IR−UV DR signals observed by probing the $(1\ 0\ 3\ 0\ 0)^0$ $J = 0$ rovibrational level are complicated by underlying IR-dark, UV-bright states, making $J = 0$ unsuitable for systematic IR−UV DR studies. The $(1\ 0\ 3\ 0\ 0)^0$ $J = 1$ rovibrational level is more amenable to unambiguous characterization and yields insight concerning even- and odd-ΔJ collision-induced rovibrational energy transfer and associated mechanisms.

I. Introduction

Collision-induced rotational and vibrational energy transfer in polyatomic molecules is a mature subject,[1,2] but it has remained of interest as our ability to carry out detailed state-to-state experiments and corresponding theory have continued to develop. For instance, the Centennial Issue of this Journal reviewed relevant aspects of vibrational energy transfer,[3] as well as related topics such as intramolecular vibrational redistribution (IVR)[4] and the vibrational predissociation dynamics of molecular clusters.[5] This paper focuses on the acetylene molecule (C_2H_2), with its characteristic linearity, central symmetry, and rich rovibrational and electronic spectroscopy. These factors result in fascinatingly complicated dynamics, much of which continues to present surprises and puzzles as fresh investigations of this ostensibly simple molecule emerge. Pages 340−364 of a recent review[6] contain a comprehensive pre-1998 bibliography on acetylene in its ground electronic state.

We use time-resolved optical double resonance (DR) spectroscopy, as depicted schematically in Figure 1. Pulsed infrared (IR) laser excitation prepares specific rovibrational states of C_2H_2 and laser-induced fluorescence (LIF) spectroscopy, with an appropriately tuned and timed ultraviolet (UV) laser pulse, is used to probe that IR excitation and subsequent rovibrational energy transfer.

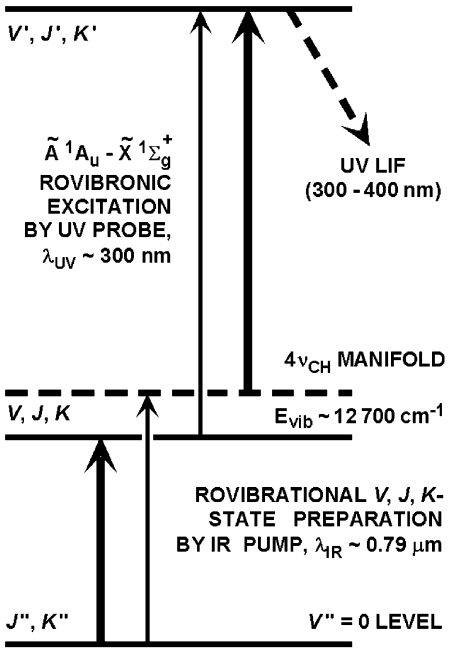

Figure 1. Excitation scheme for time-resolved, LIF-detected IR−UV DR spectroscopy of C_2H_2 in the $4\nu_{CH}$ rovibrational manifold at ∼12 700 cm^{-1}.

† Part of the special issue "Charles S. Parmenter Festschrift".

* To whom correspondence should be addressed. E-mail: brian.orr@mq.edu.au.

‡ Present address: School of Engineering and Physical Sciences, Heriot-Watt University, Riccarton, Edinburgh EH14 4AS, U.K.. E-mail: M.J.Frost@hw.ac.uk.

10.1021/jp035224t CCC: $25.00
Published on Web 10/07/2003

Our IR−UV DR spectroscopic scheme (Figure 1) is configured to investigate the energy-transfer dynamics of C_2H_2 excited to high-energy rovibrational combination/overtone levels. Here, the IR PUMP laser pulse excites a rovibrational transition $(V, J, K) \leftarrow (V'' = 0, J'', K'')$ within the electronic ground-state $\tilde{X}\ ^1\Sigma_g^+$ manifold of C_2H_2. A subsequent UV PROBE laser pulse excites a rovibronic transition $(V', J', K') \leftarrow (V, J, K)$ in the $\tilde{A}-\tilde{X}$ absorption system, detected by UV LIF from the $\tilde{A}\ ^1A_u$ electronically excited manifold. Bold and faint vertical arrows in Figure 1 indicate that some intermediate rovibrational states are IR-bright/UV-dark (i.e., prominent in the IR absorption spectrum) whereas others are IR-dark/UV-bright. Our present IR−UV DR experiments[7,8] focus on a region of the $\tilde{X}$ manifold that has vibrational energy $\omega_{vib} \approx 12\,700\ cm^{-1}$. This corresponds to a congested assembly, designated as "$4\nu_{CH}$", of rovibrational levels that are strongly perturbed from a rotating-oscillator rovibrational basis by various anharmonic, *l*-resonance, and Coriolis couplings.[6] Our IR−UV DR experiments prepare C_2H_2 molecules in a specific rotational *J*-state of that manifold.

The IR absorption band that carries most of the oscillator strength of the $4\nu_{CH}$ manifold is the combination band with the $(\nu_1 + 3\nu_3)$ zero-order label,[9−15] where ν_1 (σ_g^+) and ν_3 (σ_u^+) denote the two normal modes for CH stretching. The upper vibrational eigenstate of this band is derived from the $(1\ 0\ 3\ 0\ 0)^0\ \Sigma_u^+$ normal-mode basis state, which is estimated[7,16] at $J = 0$ to make a major (∼71%) contribution with a minor (∼21%) contribution from the $(3\ 0\ 1\ 0\ 0)^0\ \Sigma_u^+$ normal-mode basis state and the remainder from other basis states. The basis-state notation is of form $(V_1\ V_2\ V_3\ V_4\ V_5)^l$, where V_i designates vibrational quanta in each of the five normal modes $(i = 1-5)$ and *l* denotes the resultant vibrational angular momentum. Alternatively, the corresponding local-mode designation[17,18] of this submanifold is [0 4 −]. The $J = 0$ level of this IR-active $(1\ 0\ 3\ 0\ 0)^0/[0\ 4\ -]\ \Sigma_u^+$ state of the $4\nu_{CH}$ manifold is at 12 675.68 cm^{-1} (experimental[11]) or 12 674.96 cm^{-1} (calculated[16]).

Vibrational states of interest in C_2H_2 can also be classified in terms of the polyad model, introduced by Kellman et al.[19] and extensively implemented by groups such as those of Herman[6,16,20−22] and Field.[20,23−27] Vibrational manifolds are allocated three pseudo-quantum numbers: $n_s = V_1 + V_2 + V_3$; $n_{res} = 5V_1 + 3V_2 + 5V_3 + V_4 + V_5$; $l = l_4 + l_5$. The 12 675.68 cm^{-1} $(1\ 0\ 3\ 0\ 0)^0/[0\ 4\ -]\ \Sigma_u^+$ state has $n_{res} = 20$, $n_s = 4$, and $l = 1$, as do other IR-bright states of the $4\nu_{CH}$ manifold. However, many other IR-dark vibrational states, both *g* and *u*, also have $n_{res} = 20$ and $n_s = 4, 3, 2, ...$ As n_s decreases, the number of bending $(\nu_4, \pi_g; \nu_5, \pi_u)$ and CC stretching (ν_2, σ_g^+) quanta in the normal-mode basis states necessarily increases; high values of V_2 and V_4 enhance UV brightness in LIF-detected spectra and IR−UV DR signal strength. In the previously studied $\nu_{CC} + 3\nu_{CH}$ manifold,[28−31] rovibrational perturbations that conspire to enhance relative intensities in IR−UV DR spectra are localized in just a few *J*-states. On the other hand, those in the $4\nu_{CH}$ manifold[7,8,32] are more widespread. A subsequent paper[33] will examine this contrasting behavior, in terms of the polyad model.

LIF-detected IR−UV DR investigations of overtone/combination rovibrational levels at high energy (with $\omega_{vib} > 6500\ cm^{-1}$) have been reported by Crim and co-workers[34−39] and ourselves.[7,8,28−31] These have generally succeeded in resolving individual rotational *J*-states, offering insight into rotational and/or rovibrational state-to-state dynamics in relatively congested regions of the electronic ground-state ($\tilde{X}$) manifold of C_2H_2. This complements other optical double-resonance studies of collision-induced dynamics in C_2H_2 (and its isotopomers) excited to fundamental and lower overtone/combination rovibrational levels $(\omega_{vib} \leq 6500\ cm^{-1})$.[40−54] Much of our own work[7,8,28−31,40,41,43−45,47−49] has pursued the role of intramolecular perturbations in promoting (or, in some cases, inhibiting) the efficiency of rotationally selective vibrational energy transfer.[55−57]

Numerous other acetylene high-overtone experiments entail techniques such as IR absorption,[6,9−15] stimulated emission pumping (SEP),[4,58−60] dispersed LIF (both rovibronic[20,23−27,61,62] and rovibrational[63−65]), and molecular-beam laser-Stark spectroscopy.[66−68] Pulsed two-step IR−UV excitation of C_2H_2 has also been used in spectroscopic[27,69] and molecular-action[70−72] experiments.

It should be noted that the level of rovibrational excitation in our IR−UV DR experiments on the $4\nu_{CH}$ manifold $(\omega_{vib} \approx 12\,700\ cm^{-1})$ is not high enough to be regarded as "chemically significant". For instance, the barrier for isomerization from C_2H_2 to vinylidene ($H_2C{=}C{:}$) is above 15 000 cm^{-1}, with currently important dynamical implications.[73−76] We have previously proposed that some of our unusual observations in the $4\nu_{CH}$ $(\omega_{vib} \approx 12\,700\ cm^{-1})$[7,8] and $\nu_{CC} + 3\nu_{CH}$ $(\omega_{vib} \approx 11\,600\ cm^{-1})$[28−31] manifolds of C_2H_2 might be attributed to dynamical symmetry breaking, onset of isomerization, or failure of nuclear-spin-symmetry conservation. However, we have now effectively dismissed such possibilities in favor of less spectacular (but more convoluted) spectroscopic explanations, invoking a combination of Coriolis coupling (that can spoil the vibrational angular momentum quantum number *l* and give rise to odd-ΔJ rotational energy transfer, which is forbidden if $l = 0$) and significant collision-induced Stark mixing (of *g*/*u* point-group symmetry and vibrational-state character). Mechanisms of this type[8,31] will be briefly reconsidered in section VII of this paper.

Halonen and co-workers[63−65] have performed dispersed rovibrational LIF experiments, exciting C_2H_2 in the same 12 700 cm^{-1} $4\nu_{CH}$ and 11 600 cm^{-1} $\nu_{CC} + 3\nu_{CH}$ regions that have been addressed in our IR−UV DR studies.[7,8,28−31] They detect odd-ΔJ collision-induced satellite features attributed[65] to intermolecular vibrational step-down processes that effectively scramble ortho $(I = 1, a)$ and para $(I = 0, s)$ nuclear-spin modifications of C_2H_2, but without interconverting nuclear-spin states or breaking strong symmetries. This technique[63−65] is a rovibrational analogue of the vibronic LIF "chemical timing" method of Parmenter and co-workers,[77−79] except that the respective roles of collisions and intramolecular processes are reversed: timing is provided by radiative lifetime in rovibrational LIF and by collisions in vibronic LIF, whereas the phenomena of interest are collisional in rovibrational LIF and IVR in vibronic LIF. Acetylene has played a key role in parallel experiments on rovibrational energy transfer in van der Waals complexes[5] and inelastic scattering in molecular beams.[3] For instance, Miller and co-workers studied rovibrational energy disposal in the vibrational predissociation of C_2H_2-HX (X = F or Cl) van der Waals molecules.[80−82] Likewise, the classic LIF-detected experiments of Parmenter and co-workers[3,83−88] on rovibrational energy transfer in S1 glyoxal ($C_2H_2O_2$) in crossed molecular beams include C_2H_2 as a collision partner.[89]

This is our first full-length paper on IR−UV DR studies of the $4\nu_{CH}$ manifold of C_2H_2,[33] based on a dissertation by one of us.[32] Our objective is to characterize and rationalize various unusual spectroscopic and dynamical effects observed and already concisely reported.[7,8] These effects include odd-ΔJ rotational energy transfer (RET) and *J*-resolved state-to-state vibrational (V−V) energy transfer. Especially novel and challenging are collision-induced quasi-continuous background

(CIQCB) effects, underlying the discrete IR−UV DR features that are regularly observed.

In this paper, we consider IR−UV DR spectroscopic and kinetic methodology, concentrating on rotational levels in the 12 700 cm^{-1} $4\nu_{CH}$ manifold with J ranging from 0 to 12. Of particular interest here is rovibrational energy transfer involving the $J = 0$ and 1 levels of the $(1\ 0\ 3\ 0\ 0)^0/[0\ 4\ -]\ \Sigma_u^+$ submanifold of the $\tilde{X}$ state. These have been shown, by laser-Stark spectroscopy of C_2H_2 in a molecular beam,[66] to be remarkably susceptible to perturbation by an applied strong electric field (typically >200 kV cm^{-1}). The maximum Stark effect in the $4\nu_{CH}$ manifold arises through Stark mixing of the $J = 1$ level of the $(1\ 0\ 3\ 0\ 0)^0/[0\ 4\ -]\ \Sigma_u^+$ submanifold and the $J = 2$ level of an adjacent $(2\ 0\ 2\ 0\ 0)^0/[0\ 4\ +]\ \Sigma_g^+$ submanifold. The $(2\ 0\ 2\ 0\ 0)^0/[0\ 4\ +]\ \Sigma_g^+$ $J = 0$ level is slightly lower in energy than the $(1\ 0\ 3\ 0\ 0)^0/[0\ 4\ -]\ \Sigma_u^+$ $J = 0$ level; estimates of the energy difference are 4.133 ± 0.016 cm^{-1} (by Stark spectroscopy[66]), 4.052 ± 0.001 cm^{-1} (by rovibrational dispersed LIF[65]), 3.9 cm^{-1} (from local-mode calculations[18]), and 4.7 cm^{-1} (from polyad-model calculations[7]). Rotational J-levels of these respective Σ_u^+ and Σ_g^+ $4\nu_{CH}$ submanifolds − and g/u point-group symmetry − can therefore be mixed by a strong electric field, either applied or collision-induced. We have postulated[7,8,29,31] that gas-phase collisions of C_2H_2 molecules cause substantial Σ_g^+/Σ_u^+ mixing of rovibrational states, with significant implications for rovibrational state-to-state dynamics. The susceptibility for such states to become mixed in an applied or collisional electric field corresponds simply to the ease with which the relative phase of the two local CH oscillators of C_2H_2 can be switched; such a process has been suggested to be facile for transitions between some "+" and "−" local-mode states,[90] thereby mixing g/u point-group symmetry. In the $4\nu_{CH}$ manifold with $\omega_{vib} \approx 12\ 700$ cm^{-1}, collision-induced perturbations of this form are likely to occur between J-levels of the $(1\ 0\ 3\ 0\ 0)^0/[0\ 4\ -]$ and $(2\ 0\ 2\ 0\ 0)^0/[0\ 4\ +]$.[7,8] Parallel studies have been made of the $\nu_{CC} + 3\nu_{CH}$ manifold at ~11 600 cm^{-1}, in which strong Stark effects[68] arise by Σ_g^+/Σ_u^+ mixing of the $(1\ 1\ 2\ 0\ 0)^0/[0\ 3\ +]\ 1$ and $(0\ 1\ 3\ 0\ 0)^0/[0\ 3\ -]\ 1$ rovibrational submanifolds (where the local-mode notation[17,18,64,65] is now of form $[0\ V_{CH} \pm]\ V_{CC}$). This led us to postulate[31] that the $\nu_{CC} + 3\nu_{CH}$ manifold is similarly susceptible to rovibrational perturbations by collision-induced Stark fields.

II. The Central Issue: Apparently Anomalous Odd-Δ*J* RET

Figure 2 displays some representative IR−UV DR results,[7,8] in which the UV PROBE wavelength is set to monitor the $(1\ 0\ 3\ 0\ 0)^0$ $J = 1$ rovibrational level and the IR PUMP wavelength is scanned. This figure will be discussed progressively in the course of this paper. At this stage, we note that the IR absorption spectrum in trace (a) comprises the above-mentioned $(\nu_1 + 3\nu_3)$ combination band.[9−11] Trace (b) is an IR−UV DR spectrum recorded under effectively collision-free conditions with a very small Lennard-Jones collision number z; the simple two-line spectrum confirms that the IR PUMP has indeed prepared the C_2H_2 molecules in the $(1\ 0\ 3\ 0\ 0)^0$ $J = 1$ rovibrational level.

Figure 2c shows the effect of increasing the collision number z by a factor of 20, relative to Figure 2b. (As before,[7,8,28−31] values of z are referred arbitrarily to Lennard-Jones collisional rate constants k_{LJ}; for C_2H_2/C_2H_2 self-collisions at 300 K, $k_{LJ} = 16.4\ \mu s^{-1}\ Torr^{-1} = 5.10 \times 10^{-10}$ cm^3 $molecule^{-1}$ s^{-1}.) The central region of trace (c) (~12 660−12 690 cm^{-1}, for example) is dominated by customary even-ΔJ collision-induced RET

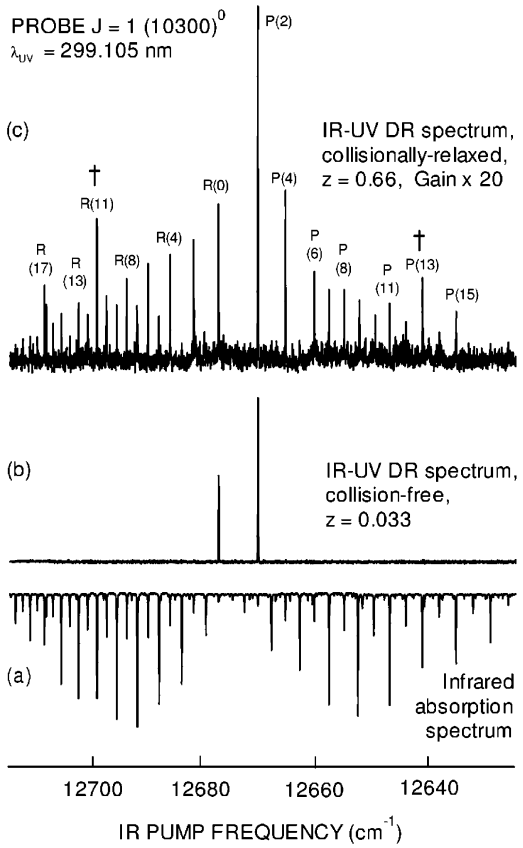

Figure 2. IR-scanned spectra of the 12 676 cm^{-1} $(\nu_1 + 3\nu_3)$ band of C_2H_2,[7,8] with R($J - 1$) and P($J + 1$) features marked: (a) photoacoustic absorption spectrum (PAS), with C_2H_2 pressure $P = 30$ Torr; (b), (c) LIF-detected IR−UV DR spectra, with the UV PROBE wavelength fixed at 299.105 nm, to monitor the $(1\ 0\ 3\ 0\ 0)^0$ $J = 1$ rovibrational level via its $\tilde{A}-\tilde{X}$ $1_1^0 3_3^1 5_0^1 K_0^1$ R(1) rovibronic transition. Lennard-Jones collision numbers z are set with $P = 200$ mTorr and varying IR−UV delay time t as follows: (b) $t = 10$ ns, $z = 0.033$; (c) $t = 200$ ns, $z = 0.66$. The collision-induced spectra in (c) are recorded with instrumental gain increased 20-fold above that for the collision-free spectrum (b). Prominent odd-ΔJ R(11) and P(13) RET satellites are marked with a dagger.

satellites, as is expected for a centrosymmetric linear molecule such as C_2H_2. However, the wings of this spectrum contain an additional set of anomalous odd-ΔJ collision-induced satellites. These are centered around the R(11) and P(13) "$J = 12$ to $J = 1$" IR−UV DR features (marked with daggers) that have the $(1\ 0\ 3\ 0\ 0)^0$ $J = 12$ rovibrational level in common.

The mechanism of this odd-ΔJ RET behavior[7,8] seems, at least prima facie, to fail to conserve a/s nuclear-spin symmetry. A central theme of this paper is to seek plausible explanations for apparent anomalies such as this. It is necessary to take care to eliminate (or at least identify) trivial effects that may mask physically significant processes: for instance, accidental coincidences of more than one spectroscopic transition at a particular IR PUMP or UV PROBE wavelength, of which there are examples in sections IV and V below. The need for careful, systematic investigations is well illustrated in section V, where IR−UV DR spectra, ostensibly associated with the $(1\ 0\ 3\ 0\ 0)^0$ $J = 0$ rovibrational level, are shown to be greatly complicated by the presence of other masking states.

In this context, we note that our IR−UV DR measurements involve three key experimental factors: IR PUMP wavelength, UV PROBE wavelength, and IR−UV delay t (or collision number z). It is therefore possible to define three distinct varieties of IR−UV DR experiment:

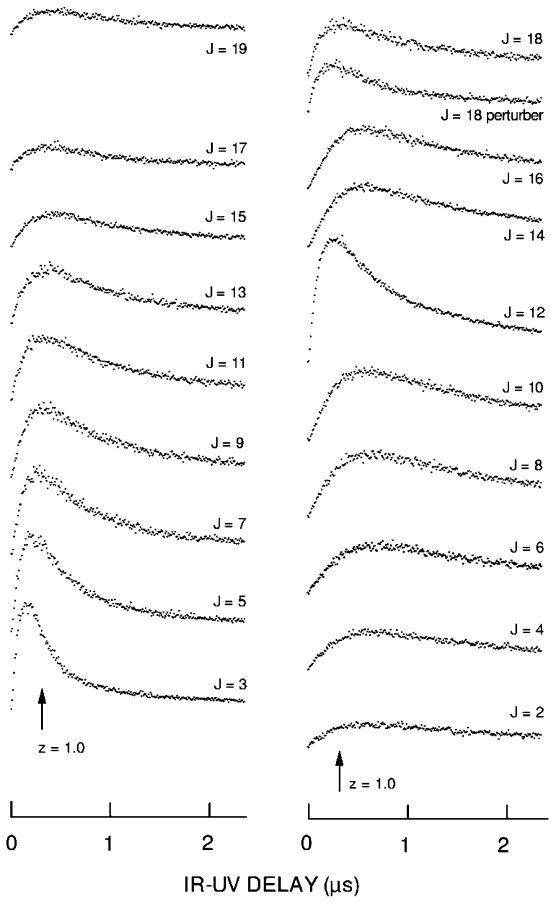

Figure 3. Averaged IR−UV DR kinetic curves for C_2H_2 ($P = 200$ mTorr), with the 299.105 nm UV PROBE monitoring the $(1\ 0\ 3\ 0\ 0)^0$ $J = 1$ level and the IR PUMP set to monitor the kinetics of both even-ΔJ RET (left-hand column) and odd-ΔJ RET (right-hand column) over the range $J = 2-19$.

(i) *IR-scanned IR−UV DR spectra* (e.g., as in Figure 2 above), in which the UV PROBE wavelength and z (i.e., P and t) are fixed while the IR PUMP wavelength is tuned;

(ii) *UV-scanned IR−UV DR spectra* (e.g., as in section IV below), in which the IR PUMP wavelength and z (i.e., P and t) are fixed while the UV PROBE wavelength is tuned;

(iii) *IR−UV DR kinetic scans* (e.g., as in Figure 3), in which IR−UV delay t (and hence z) are scanned while the sample pressure P and IR PUMP and UV PROBE wavelengths are fixed.

Each of these IR−UV DR schemes depends on which one of the three experimental factors is continuously varied while the other two are held fixed. They reveal particular spectroscopic or collision-induced processes by stepwise variation of settings for either of the two "fixed" factors between successive IR−UV DR scans. For instance, Figure 2 shows how IR-scanned IR−UV DR spectra vary markedly with successive settings of IR−UV time delay t (and hence z, for fixed sample pressure P) with the UV PROBE set at a characteristic wavelength.

Figure 3 shows corresponding IR−UV DR kinetic results, in which the UV PROBE set at 299.105 nm monitors the $(1\ 0\ 3\ 0\ 0)^0$ $J = 1$ level and the IR PUMP prepares various J-levels. Vertical arrows mark the value of t at which gas-kinetic ($z = 1.0$) collisional conditions apply. The kinetic curves are arranged in two columns, with the regular even-ΔJ RET on the left and supposedly forbidden odd-ΔJ RET on the right. A remarkable feature is the prominence of the "$J = 12$ to $J = 1$" odd-ΔJ RET channel (labeled "$J = 12$" in the right-hand column of Figure 3), for which the IR−UV DR kinetic efficiency is comparable to that for the regular $|\Delta J| = 2$ and $|\Delta J| = 4$ RET channels ("$J = 3$" and "$J = 5$" respectively in the left-hand column of Figure 3). This "$J = 12$ to $J = 1$" odd-ΔJ RET channel is consistent with the IR-scanned IR−UV DR spectrum shown in Figure 2c. Other odd-ΔJ RET features fall away monotonically from the kinetic curve for $J = 12$, as if from a secondary parent peak. The level labeled "$J = 18$ perturber" is associated with the lower-energy component of the locally perturbed R(17) doublet at ~12 709.3 cm^{-1} in Figure 2.[9,11−13,15] Such kinetics of individual collision-induced IR−UV DR features reveals apparent symmetry-breaking IR−UV DR signals originating from even-J levels of $(1\ 0\ 3\ 0\ 0)^0$ (notably $J = 12$) when the $(1\ 0\ 3\ 0\ 0)^0$ $J = 1$ level is probed. Figure 3 is representative of an extensive body of IR−UV DR kinetic results that can be satisfactorily simulated by a phenomenological master-equation model.[32,33]

The majority of IR−UV DR measurements presented in this paper are performed with the UV PROBE tuned to the 299 nm $\tilde{A}-\tilde{X}$ $1_1^0 3_3^1 5_0^1$ rovibronic absorption band, whereas a limited number of experiments have the UV PROBE tuned to the 296 nm $\tilde{A}-\tilde{X}$ $1_1^0 2_0^1 3_3^0 5_0^1$ band. Systematic UV-scanned IR−UV DR measurements, described in section IV, offer insight into the rovibrational character of the intermediate $\tilde{X}$-state levels that are excited by IR PUMP absorption in our experiments. For instance, relative intensities in UV-scanned IR−UV DR spectra reflect the Σ, Π, Δ, ... ($l = 0, 1, 2, ...$) character of the $\tilde{X}$-state rovibrational levels involved; such information is crucial to odd-ΔJ RET mechanisms that are briefly considered in section VII. Reduced term-value plots can help to characterize the upper vibronic levels of the $\tilde{A}$-state manifold accessed by $\tilde{A}-\tilde{X}$ IR−UV DR absorption and this, in turn, provides clues about the symmetry of the intermediate rovibrational levels of the $\tilde{X}$ manifold that are prepared by the IR PUMP.

Subsequent papers in this series[33] will explore the apparent energy-transfer gateway at $J = 12$. They will also seek explanations of the unusual CIQCB effects[8,32] that underlie most of our $4\nu_{CH}$ IR−UV DR experiments, present additional IR−UV DR results for rovibrational levels with $J > 12$, and formulate spectroscopic and kinetic models of observed results. In the meantime, this paper lays foundations in terms of our IR−UV DR investigations of low-J rovibrational levels ($J \leq 12$).

III. IR−UV DR Experimental Procedures

Our apparatus for time-resolved, LIF-detected IR−UV DR spectroscopy is illustrated in Figure 4. Our IR−UV DR techniques have been described elsewhere;[7,8,28−32] they are similar to those of Crim and co-workers.[35,36] Specific information and significant technical improvements are discussed below. Recent variants of our IR−UV DR apparatus have used solid-state nonlinear-optical and laser devices (such as optical parametric oscillators) to generate pulsed IR PUMP and UV PROBE radiation with higher spectroscopic resolution.[32,91] However, such refinements have not been used to gather any of the results reported in this paper.

In Figure 4, pulsed IR PUMP radiation at ~790 nm is generated by Raman-shifting tunable visible light at ~595 nm from a Nd:YAG-pumped dye laser system (Continuum models NY61 and ND60, with mixed Rhodamine B and 101 dyes in methanol). The Raman shifter (Quanta-Ray model RS-1) uses hydrogen gas at ~7.5 bar and a backward-scattered geometry; it generates phase-conjugate first-Stokes radiation at ~790 nm with 8−10 mJ per 7 ns pulse, an optical bandwidth of ~0.08

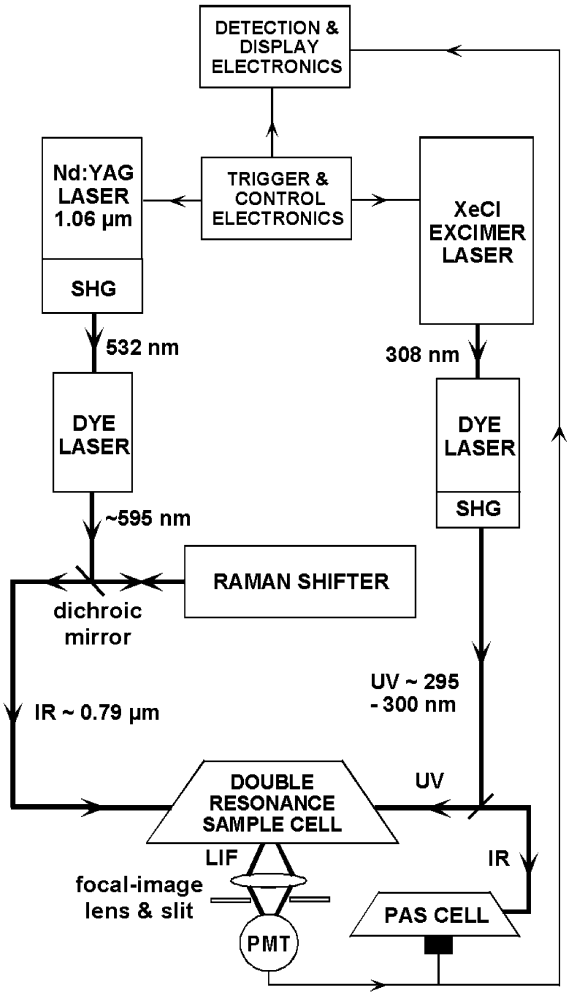

Figure 4. Apparatus layout for IR−UV DR spectroscopy: LIF = laser-induced fluorescence; PAS = photoacoustic spectroscopy; PMT = photomultiplier tube; SHG = second-harmonic generator.

cm^{-1}, and good beam quality (comparable to that of the dye laser input). Signals from a separate photoacoustic absorption spectroscopy (PAS) cell, containing C_2H_2 gas at ~30 Torr, are also monitored to yield reference IR absorption spectra whenever the IR PUMP wavelength is tuned (e.g., as in Figure 2).

The UV PROBE radiation is generated by a frequency-doubled, XeCl excimer-pumped dye laser system (Lambda-Physik models LPX100 and FL3002E); typically, it comprises ~0.5 mJ per 15 ns pulse, with an optical bandwidth of ~0.2 cm^{-1}. The UV PROBE wavelength is tuned to one of the two distinct vibronic bands in the $\tilde{A}-\tilde{X}$ absorption system of C_2H_2 that are of primary interest in this paper:[7,8,32] *either* the $1^0_1 3^1_3 5^1_0$ band at ~299 nm *or* the nearby $1^0_1 2^1_0 3^0_3 5^1_0$ band at ~296 nm. Other UV wavelengths (notably ~323 nm) have been used in experiments that are reported elsewhere.[32,33]

The counter-propagating IR PUMP and UV PROBE beams are linearly polarized in the horizontal plane; they overlap in a common focal zone, from which UV LIF is collected, at the center of a cylindrical optical cell fitted with Brewster-angle windows and a train of light baffles. The cell contains C_2H_2 gas (either neat or mixed in known proportions with a buffer gas such as argon) at a known temperature *T* and pressure *P* (typically ~100 mTorr, measured by an electronic manometer). The cell has a side-window, through which broadband LIF light from the focal zone is collected to monitor the molecular processes initiated by IR−UV DR excitation. The LIF light is imaged by a silica lens, spatially filtered by a horizontal slit (to minimize background scattered light), spectrally filtered to select UV wavelengths longer than that of the UV PROBE at ~300 nm, and detected by a photomultiplier (Hamamatsu 1P28). Electronic processing by a fast preamplifier and boxcar integrator (Stanford Research Systems models SR445 and SR245) is gated to exclude the initial 25 ns period after the UV PROBE pulse, to which most of the unwanted background noise is confined.

Accurate timing of the interval *t* between IR PUMP and UV PROBE pulses is controlled by a digital delay generator (Stanford Research Systems model DG535) and monitored by a universal counter (Hewlett-Packard model 5328A), yielding a time resolution of ±10 ns.[30] Most key instrumental functions, notably tuning and timing of IR PUMP and UV PROBE pulses and acquisition of UV LIF and PAS signals, are registered by computer over an IEEE−488 data bus. Such measures ensured that IR−UV DR kinetic data, collected progressively over several months, were internally self-consistent with respect to IR−UV DR signal amplitude, allowing reliable comparison of kinetic curves for different features in the overall data set, as is evident from Figure 3.

IV. Preliminary Spectroscopic Surveys

The $4\nu_{CH}$ region of C_2H_2 at ~12 700 cm^{-1} (~0.79 μm) comprises several IR absorption bands including the main $(\nu_1 + 3\nu_3)$ $\Sigma_u^+ - \Sigma_g^+$ band.[9−12] In a previous study, Tobiason et al.[35,92] found that $(1\ 0\ 3\ 0\ 0)^0$ rovibrational levels were particularly amenable to investigation by IR−UV DR methods. In that work, UV-scanned IR−UV DR spectra were recorded for selected *J*-levels of the $(1\ 0\ 3\ 0\ 0)^0$ submanifold in the 299 nm $\tilde{A}-\tilde{X}$ $1^0_1 3^1_3 5^1_0$ rovibronic absorption band[92] and total collision-induced relaxation rates were measured for the $J = 0$, 4, 10, and 18.[35] Our IR−UV DR studies in this region extend that earlier work, by examining many more *J*-levels (up to $J = 22$) of the $(1\ 0\ 3\ 0\ 0)^0$ submanifold and by investigating state-to-state collision-induced rovibrational energy transfer.

When the collision number *z* is small, as in Figure 2b, the only IR−UV DR features that appear in a UV-probed spectrum are those from the same rovibrational level (*V, J, K*) that is directly excited at the (fixed) IR PUMP wavelength. UV-scanned IR−UV DR spectra of this form, recorded under effectively collision-free conditions ($z = 0.016$), are presented in Figure 5. If *z* is allowed to increase, as in the parallel IR-scanned and kinetic cases of Figures 2c and 3, additional structure grows into the UV-scanned IR−UV DR spectrum as collision-induced relaxation occurs within the manifold of rovibrational levels (*V, J, K*). It should be noted that the vibronic bands in UV-scanned IR−UV DR spectra are hot bands originating in high overtone/combination levels, so that they are not seen in conventional UV absorption spectra. However, they can often be identified by combination-difference methods. The set of survey spectra shown in Figure 5 was recorded, as a prerequisite for further IR−UV DR studies, with the IR PUMP preparing successive *J*-levels of the $(1\ 0\ 3\ 0\ 0)^0$ submanifold by setting its wavelength on corresponding $P(J + 1)$ and $R(J - 1)$ features of the $(\nu_1 + 3\nu_3)$ absorption band of C_2H_2. A similar, but less extensive, set of spectra has been presented by Tobiason.[92]

The vibronic band in Figure 5 is denoted $1^0_1 3^1_3 5^1_0$, with the $(\nu'_3 + \nu'_5)$ upper vibronic state (i.e., $V'_3 = 1$, $V'_5 = 1$) selected by scanning the UV PROBE wavelength in the 299 nm region. Each trace shows the characteristic $\tilde{A}-\tilde{X}$ $1^0_1 3^1_3 5^1_0$ band rovibronic spectrum for a particular *J* value, ranging from 0 to 18,

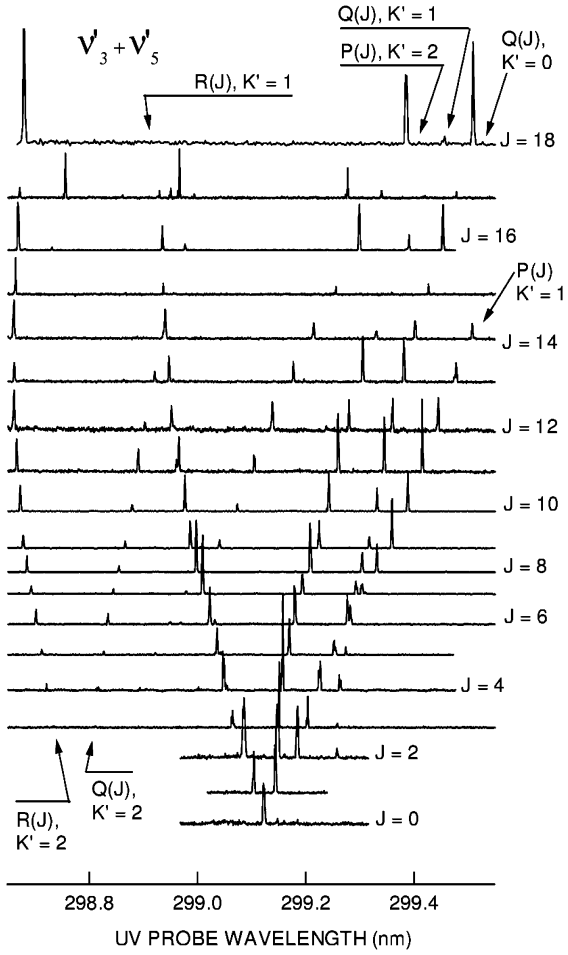

Figure 5. UV-scanned IR−UV DR survey spectra for C_2H_2 prepared by the IR PUMP in $(1\ 0\ 3\ 0\ 0)^0$ rovibrational levels with $J = 0-18$. The UV PROBE is scanned through the $\tilde{A}-\tilde{X}\ 1^0_1 3^1_3 5^1_0$ rovibronic band at ~299 nm, exciting the $(\nu'_3 + \nu'_5)$ upper vibronic state. All spectra are recorded with C_2H_2 pressure $P = 100$ mTorr, IR−UV DR delay $t = 10$ ns, and $z = 0.016$.

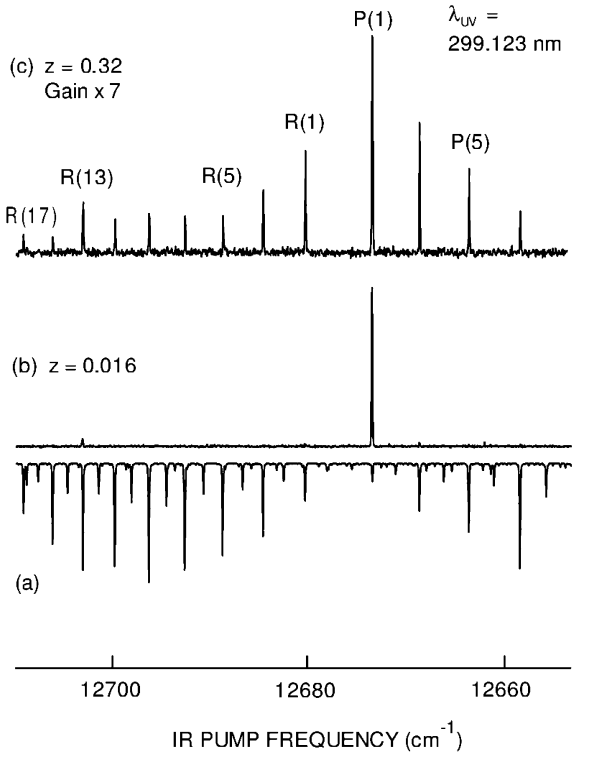

Figure 6. IR-scanned spectra of C_2H_2 similar to Figure 2, except that the UV PROBE wavelength is fixed at 299.123 nm to monitor the $(1\ 0\ 3\ 0\ 0)^0$ $J = 0$ rovibrational level. The IR−UV DR spectra are recorded with $P = 100$ mTorr and (b) $t = 10$ ns, $z = 0.016$ and (c) $t = 200$ ns, $z = 0.32$.

and with values of K' marked on the spectra. The survey spectra in Figure 5 are recorded with moderate instrumental gain, so that additional, weaker rovibronic features arise when higher sensitivity is used. The primary subbands in Figure 5 are $1^0_1 3^1_3 5^1_0\ K^1_0$ (i.e., $K' = 1 \leftarrow K = l = 0$). Even-$K'$ features with $K' = 0$ and $K' = 2$ also occur; at higher J (>10, for example), these may arise from axis switching,[43,93,94] but at low J, they indicate key perturbations in the rovibrational state that mix in odd values of l (=K), notably $l = 1$,[8,29,31] spoiling l as a "good" quantum number. Assignment is facilitated by reduced term-value plots[95,96] to identify K' and correlate P, Q, and R branches of the rotational structure.[32,92] Not all of the rovibronic features in Figure 5 can be identified, suggesting the presence of IR-dark states (as shown in Figure 1), excited at the particular IR PUMP wavelength; these may be avoided by switching between alternative P($J + 1$) and R($J - 1$) IR wavelengths.

A second, less extensive set of UV-scanned IR−UV DR spectra has also been recorded (but not presented here)[32,33] for the 296 nm $\tilde{A}-\tilde{X}\ 1^0_1 2^1_0 3^0_3 5^1_0$ rovibronic band, with the $(\nu'_2 + \nu'_5)$ upper vibronic state (i.e., $V'_2 = 1$, $V'_5 = 1$). IR−UV DR spectra detected via this alternative $(\nu'_2 + \nu'_5)$ upper vibronic state present interesting contrasts with those detected at ~299 nm (as in Figures 2, 3, and 5) via $(\nu'_3 + \nu'_5)$, as will be reported in sections VI and VII.

UV-scanned IR−UV DR spectra, as in Figure 5, can determine whether a given IR−UV DR rovibronic feature is uniquely characteristic of its designated rovibrational J-state. This is not always the case, as we have already reported[7] in the case of an accidental coincidence at 299.145 nm between rovibronic features associated with $J = 1$ and $J = 12$. In the two-line spectrum for $J = 1$ in Figure 5, the shorter-wavelength R(1) feature at 299.105 nm has no such accidental interference and can be used for systematic IR−UV DR studies.[7] In corresponding IR−UV DR spectra that are detected by means of the 296 nm $\tilde{A}-\tilde{X}\ 1^0_1 2^1_0 3^0_3 5^1_0$ rovibronic band, both R(1) and P(1) features appear[32,33] to be clear of interferences from features of $J = 12$ or any other J states represented here.

We emphasize that it is essential to search carefully for possible spectroscopic ambiguities such as these, to make reliable interpretations of IR−UV DR spectra, with respect to less trivial molecular phenomena such as odd-ΔJ RET and V−V transfer.

V. Probing the $(1\ 0\ 3\ 0\ 0)^0$ $J = 0$ Level

Our systematic approach to IR−UV DR investigations of spectra and energy transfer is illustrated by experiments in which the UV PROBE wavelength is tuned to the vicinity of 299.123 nm. Three IR-scanned spectra in this domain are shown in Figure 6.

The UV PROBE then accesses the R(0) rovibronic feature of the $\tilde{A}-\tilde{X}\ 1^0_1 3^1_3 5^1_0\ K^1_0$ subband (as shown in the lowest trace of Figure 5), thereby probing the $J = 0$ rovibrational level. Figure 6a is a PAS reference scan, showing the central portion of the $(\nu_1 + 3\nu_3)$ IR absorption band of C_2H_2.[9−11] This exhibits the characteristic 3:1 intensity alternation between odd-J'' and even-J'' features due to the nuclear-spin statistics of the centrosymmetric C_2H_2 molecule. Figure 6b,c are corresponding

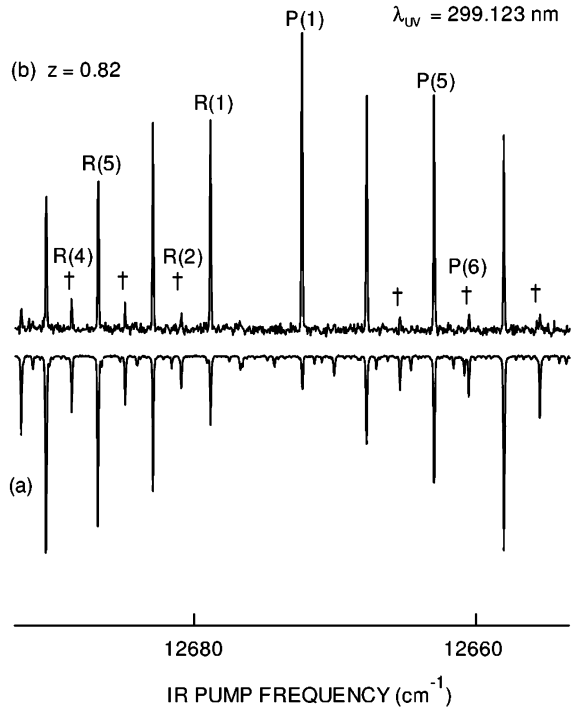

Figure 7. IR-scanned spectra of C_2H_2 similar to Figure 6, except that $P = 500$ mTorr, $t = 200$ ns, and $z = 0.82$. Weak odd-ΔJ RET features are marked with a dagger.

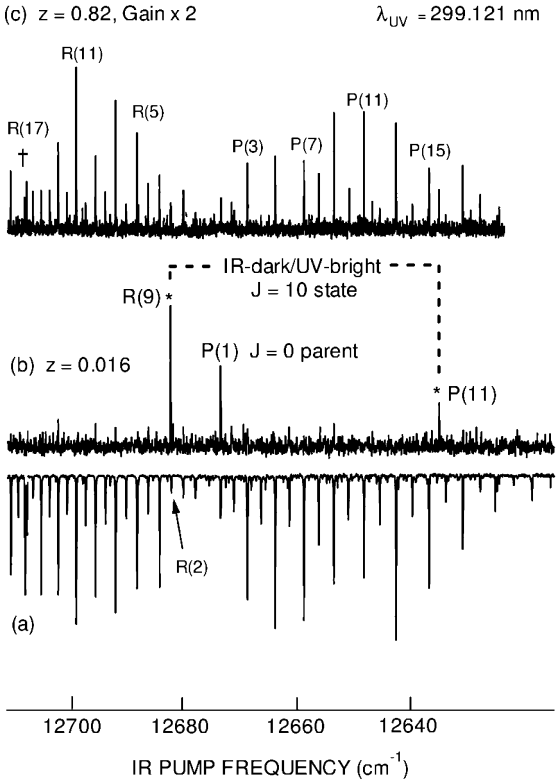

Figure 8. IR-scanned spectra of C_2H_2 similar to Figure 6, except that the UV PROBE wavelength is shifted to 299.121 nm, where new odd-ΔJ IR−UV DR features (asterisked) appear.

IR−UV DR spectra, recorded by scanning the IR PUMP wavelength with the UV PROBE wavelength fixed at 299.123 nm to monitor the $(1\ 0\ 3\ 0\ 0)^0$ $J = 0$ level via its $\tilde{A}-\tilde{X}$ $1_1^0 3_3^1 5_0^1$ K_0^1 R(0) rovibronic transition. Trace (b) is recorded under effectively collision-free conditions ($z = 0.016$) and comprises a single prominent line: the expected 12 673.28 cm^{-1} P(1) peak of the $(\nu_1 + 3\nu_3)$ band. In trace (c), which is recorded with collision number z and instrumental gain increased 20-fold and 7-fold, respectively, an array of even-ΔJ RET satellites are now evident. Closer inspection of Figure 6b reveals a very weak IR−UV DR parent peak corresponding to the $(\nu_1 + 3\nu_3)$ R(13) feature. This is attributed to an overlapping rovibronic feature in the $\tilde{A}-\tilde{X}$ $1_1^0 3_3^1 5_0^1$ band associated with $J = 14$ (too weak to discern in the $J = 14$ trace of Figure 5), falling within the optical bandwidth of the UV PROBE laser. This secondary $J = 14$ IR−UV DR feature is also evident in Figure 6c, where the R(13) peak is more prominent than its neighbors. An extension of Figure 6 is shown in Figure 7, where collision number z in trace (b) has been increased 50-fold relative to that in Figure 6b.

Even-ΔJ RET satellites are more prominent in Figure 7b than in Figure 6c. More remarkably, we see a series of supposedly forbidden satellites (daggered) that indicate dynamically significant collision-induced odd-ΔJ RET, as found in other contexts.[7,8,28−31] We have sought, but have not found, a trivial explanation for these odd-ΔJ RET satellites. For instance (as explained below), although there is an interference from an even-J rovibronic transition within the UV PROBE optical bandwidth, there is no corresponding odd-J interference (such as has been used to explain similar effects seen[37] by IR−UV DR in the 9600 cm^{-1} $3\nu_3$ region). In attempts to locate IR−UV DR parent features associated with rovibrational states (most likely IR-dark) with UV PROBE transitions within the optical bandwidth (≥ 0.2 cm^{-1} fwhm) of the UV PROBE laser, we have recorded successive IR-scanned IR−UV DR spectra with the UV PROBE detuned stepwise from the wavelength of 299.123 nm that is optimal for monitoring the $(1\ 0\ 3\ 0\ 0)^0$ $J = 0$ level, as in Figure 8.

Parts b and c of Figure 8 show what happens if the UV PROBE wavelength is reduced by 0.002 nm (~ 0.22 cm^{-1}). The P(1) IR−UV DR parent peak in Figure 8b has a poorer signal-to-noise ratio than in Figure 6b (as the UV PROBE is detuned from the $J = 0$ rovibronic peak), but there are two previously unobserved parent peaks, asterisked in Figure 8b. The interval between the asterisked peaks in trace (b) is that expected for a $J = 10$ level, suggesting that they arise from an unidentified IR-dark/UV-bright $J = 10$ rovibrational state, with an optimal UV PROBE wavelength of 299.121 nm. This is confirmed by setting the IR PUMP wavelength on either of these peaks and scanning the UV PROBE wavelength, as in Figure 9a,b, which are low-z, UV-scanned IR−UV DR spectra corresponding respectively to the asterisked R(9) and P(11) peaks of Figure 8b. They are virtually identical, confirming that the asterisked peaks in Figure 8b share a common rovibrational level. Figure 9c shows a template for $(\nu'_3 + \nu'_5)$ $\tilde{A}$-state rovibronic levels UV-excited from a $J = 10$ rovibrational level; it comprises the $1_1^0 3_3^1 5_0^1$ band rovibronic spectrum for $J = 10$ from Figure 5, translated by 14.5 cm^{-1} to coincide with the UV LIF excitation frequency scale of traces (a) and (b). The similarity between Figure 9a−c confirms that the new rovibrational level corresponds to $J = 10$, approximately 14.5 cm^{-1} lower in energy than the IR-bright $(1\ 0\ 3\ 0\ 0)^0$ $J = 10$ level.

Polyad-model calculations[31,33] suggest that the vibrational eigenstate to which the IR-dark $J = 10$ level belongs is most likely to have $(0\ 3\ 1\ 6\ 0)^0$ Σ_u^+ as its dominant normal-mode basis state, with pseudo-quantum numbers $n_s = 4$, $n_{res} = 20$, and $l = 0$ (as for IR-bright components of the $4\nu_{CH}$ polyad). The many CC stretching and trans-bending quanta are consistent with the UV brightness of this level, whereas its complexity should make it IR-dark. There is no vestige of the IR-dark $J =$

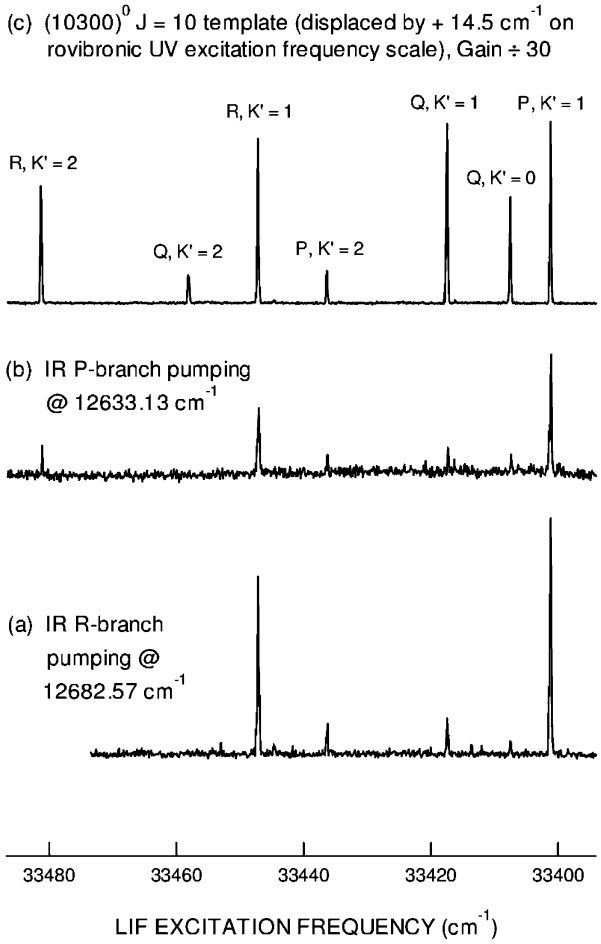

Figure 9. UV-scanned $J = 10$ IR−UV DR spectra for C_2H_2, with the UV PROBE scanned in the vicinity of the 299 nm $\tilde{A}-\tilde{X}$ $1_1^0 3_3^1 5_0^1$ band, as in Figure 5. Traces (a) and (b) are recorded with the IR PUMP tuned to each of the asterisked features in Figure 8b. Trace (c) is the $1_1^0 3_3^1 5_0^1$ band rovibronic spectrum for $J = 10$, translated as a template from Figure 5.

10 state in IR absorption spectra of C_2H_2, such as the PAS scan in Figure 8a, nor is it seen in IR−UV DR spectra at higher z, or if the UV PROBE wavelength is tuned away from 299.121 nm.

The collision-induced IR−UV DR spectrum in Figure 8c merits close scrutiny, for it displays several features that have significant dynamical implications. One is that the envelope of even-J'' and odd-J'' rovibrational peaks is much closer to the thermally equilibrated intensity distribution in IR spectra, as in Figure 8a, than it was in Figure 7b where odd-J'' peaks (arising from even-ΔJ RET) roll off in ampitude from that of the P(1) (i.e., $J = 0$) parent peak and are much more prominent than the even-J'' peaks (daggered, arising from odd-ΔJ RET). Moreover, the amplitude of the P(1) IR−UV DR parent peak in the collision-free spectrum of Figure 8b is insufficient to account for the total integrated intensity of the collision-induced IR−UV DR spectrum in Figure 9c. It seems that there is a source of collision-induced IR−UV DR signal amplitude additional to that arising regularly through even-ΔJ RET from the parent IR−UV DR spectrum observed at low z. We intend to explain these observations, in terms of CIQCB effects,[8,32] in a subsequent paper.[33]

The IR-dark, UV-bright $J = 10$ features of Figure 8b arise simply from an accidental coincidence (within ~0.2 cm^{-1}) with the sole $(1\ 0\ 3\ 0\ 0)^0$ $J = 0$ P(1) feature in the UV-scanned IR−UV DR spectrum of C_2H_2. There is no suggestion that they arise from a local perturbation. A classic example of a local perturbation in the $4\nu_{CH}$ manifold occurs for the $(1\ 0\ 3\ 0\ 0)^0$ $J = 17$ and $J = 18$ levels, as is evident from doublet structure in the corresponding $(\nu_1 + 3\nu_3)$ band;[9,11−13,15] the prominent R(17) doublet in Figures 2, 6, and 8 is at ~12 709.45 and ~12 709.1 cm^{-1} (perturber). It is noteworthy (but, at this stage inexplicable) that the amplitude ratio of the collision-induced $J = 18$ doublet feature, marked by a dagger at R(17) in Figure 8c, is unusual. In virtually all of our other IR−UV DR spectra (for instance, Figures 2c and 6c) this ratio is similar to that in the corresponding IR absorption spectrum (Figures 2a and 6a). By contrast, the amplitude ratio for the daggered R(17) doublet in Figure 8c is reversed relative to that in Figure 8a. We believe that this is a significant observation, but its mechanistic implications are not yet clear.

As explained in section I above, the attention of our IR−UV DR experiments was originally attracted to the $(1\ 0\ 3\ 0\ 0)^0$ $J = 0$ level on the basis of its anomalously large Stark effect[66] and the likelihood that this would therefore be amenable to collision-induced Stark effects that could mix *g*/*u* point-group symmetry and effectively facilitate energy transfer between "+" and "−" local-mode states.[90] Such mechanisms may well be in operation in the context of the $(1\ 0\ 3\ 0\ 0)^0$ $J = 0$ level, particularly with regard to the appearance of collision-induced odd-ΔJ IR−UV DR features as in Figures 7b and 8c. However, only one UV PROBE wavelength (~299.123 nm) is available to monitor the $(1\ 0\ 3\ 0\ 0)^0$ $J = 0$ level, because no P- or Q-branch rovibronic transition is allowed from $J = 0$ in the $1_1^0 3_3^1 5_0^1$ K_0^1 band. Moreover, resulting IR-scanned IR−UV DR spectra are complicated by interferences from two other directly excited rovibrational states: a weak contribution from the $(1\ 0\ 3\ 0\ 0)^0$ $J = 14$ level, as in Figure 6b,c, and the slightly off-resonant intrusion of an IR-dark $J = 10$ level, as in Figure 8b. Fortuitously, both of these extra directly excited rovibrational levels have even J (and, presumably, the same *ungerade* point-group symmetry), so that they do not detract from the significance of collision-induced odd-ΔJ RET structure, as in Figures 7c and 8c. Nevertheless, they impose complications that discourage more detailed studies of odd-ΔJ RET effects by IR−UV DR spectra with the UV PROBE monitoring the $(1\ 0\ 3\ 0\ 0)^0$ $J = 0$ level. The $(1\ 0\ 3\ 0\ 0)^0$ $J = 1$ level (which is also susceptible to strong Stark mixing[66]) has proved to be a far more fertile subject area,[7,8] as is demonstrated in the next section.

VI. Probing the $(1\ 0\ 3\ 0\ 0)^0$ $J = 1$ Level

We now return to IR-scanned IR−UV DR spectra of C_2H_2 in which the UV PROBE monitors the $(1\ 0\ 3\ 0\ 0)^0$ $J = 1$ level. This was central to two previous papers[7,8] and was previewed in Figures 2 and 3 above. We now provide additional details and further insight. Figure 2 shows two IR-scanned IR−UV DR spectra together with a corresponding PAS reference scan. The central portion of Figure 2, between the R(4) and P(6) features, exhibits "well behaved" even-ΔJ RET satellites as z increases. The higher-J portions of the collision-induced spectra are complicated by additional, supposedly forbidden odd-ΔJ RET satellite structure, centered around $J = 12$. The IR−UV DR spectra in Figure 2b,c were obtained with the UV PROBE wavelength fixed on the 299.105 nm R(1) $K' = 1$ feature (i.e., K_0^1 subband) of the $\tilde{A}-\tilde{X}$ $1_1^0 3_3^1 5_0^1$ rovibronic band and scanning the IR PUMP wavelength through the $(\nu_1 + 3\nu_3)$ IR absorption band. As explained in section IV above and elsewhere,[7] this choice of UV PROBE wavelength avoids interferences from other overlapping rovibrational states such as were encountered in the case of $J = 0$ in section V above.

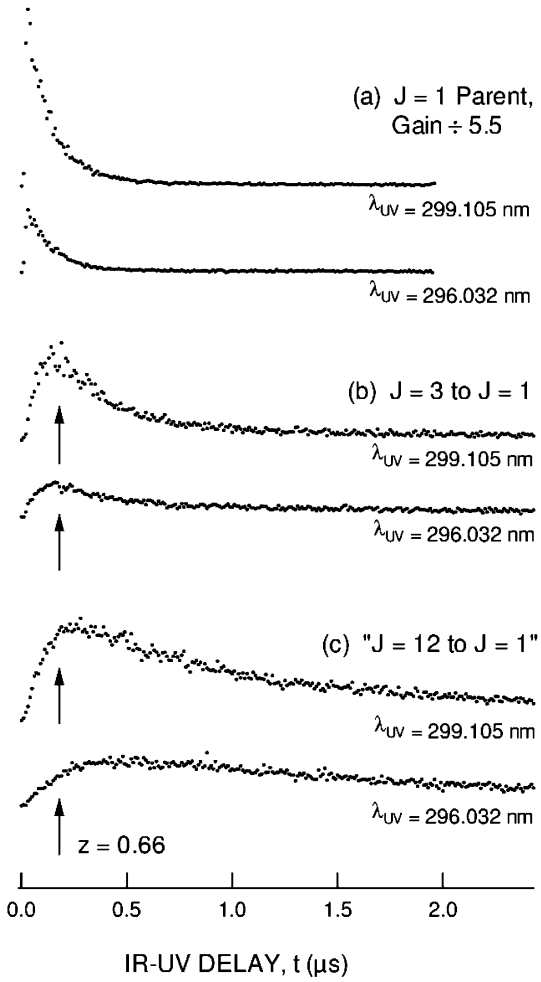

Figure 10. IR−UV DR kinetic curves for $(1\,0\,3\,0\,0)^0$ $J = 1$ population in C_2H_2 ($P = 200$ mTorr). For the upper curve of each pair, the UV PROBE is set at 299.105 nm (as in Figure 2); in the lower, it is at 296.032 nm (as in Figure 1 of ref 8). The IR PUMP is set to monitor the kinetics of (a) the $(1\,0\,3\,0\,0)^0$ $J = 1$ parent, (b) "$J = 3$ to $J = 1$" $|\Delta J| = 2$ RET, and (c) "$J = 12$ to $J = 1$" odd-ΔJ RET.

As outlined in section II, the central portions of Figure 2b,c are classic rotationally selective IR−UV DR spectra, apparently uncomplicated by effects such as odd-ΔJ RET. However, the higher-J collision-induced wings of Figure 2c exhibit odd-ΔJ features that are most prominent for the asterisked $J = 12$ peaks. This implies that a facile collision-induced RET process with $\Delta J = -11$ is populating the $J = 1$ level monitored by the UV PROBE.[7,8]

Similar (but not identical) odd-ΔJ RET effects are apparent when a different UV PROBE wavelength is used to excite another upper vibronic state. We have previously reported[8] that there are apparently negligible differences between IR-scanned IR−UV DR spectra, each monitoring the $(1\,0\,3\,0\,0)^0$ $J = 1$ level, with UV PROBE wavelengths of 299.105 nm (accessing the $(\nu'_3 + \nu'_5)$ upper vibronic state, as in Figure 2) and 296.032 nm (exciting the R(1) $K' = 1$ feature of the $\tilde{A}-\tilde{X}$ $1^0_1 2^1_0 3^0_3 5^1_0$ K^1_0 rovibronic band to access $(\nu'_2 + \nu'_5)$, as in Figure 1 of ref 8).

A quantitative investigation of this situation has been made by recording IR−UV DR kinetic curves, as shown in Figure 10. This comprises three pairs of IR−UV DR kinetic curves; the upper curve of each pair corresponds to $(1\,0\,3\,0\,0)^0$ $J = 1$ population monitored with the UV PROBE set at 299.105 nm (as in Figure 2) and the lower at 296.032 nm (as in Figure 1 of ref 8). Each kinetic curve is digitized and averaged (over ~30 laser shots per data point) as the IR−UV delay t is continuously scanned. Vertical arrows mark the collision number ($z = 0.066$) at which the two forms of IR-scanned IR−UV DR spectra were recorded.[7,8] The two traces in Figure 10a, for $(1\,0\,3\,0\,0)^0$ $J = 1$ parent kinetics, and those in Figure 10b, depicting regular "$J = 3$ to $J = 1$" $|\Delta J| = 2$ RET kinetics, differ little within each pair, apart from overall amplitude variations associated with different cross-sections for UV absorption and LIF. They are consistent with growth of collision-induced even-ΔJ satellites in corresponding IR-scanned IR−UV DR spectra, as in Figure 2 and our earlier work.[7,8] However, the two kinetic curves depicted in Figure 10c differ appreciably, contrary to the previously reported similarity[8] of corresponding IR-scanned IR−UV DR spectra.

It seems that "$J = 12$ to $J = 1$" odd-ΔJ RET contains a fast kinetic component that is more prominent when the UV PROBE is at 299.105 nm than when it is at 296.032 nm. It may be that the rovibrational levels probed (particularly $J = 12$) have vibrational basis states with stronger vibronic transition probability to the $(\nu'_3 + \nu'_5)$ upper state than to $(\nu'_2 + \nu'_5)$. We have evidence[8] that more than just a single discrete set of $(1\,0\,3\,0\,0)^0$ J states contributes to IR−UV DR spectra and kinetics of the $4\nu_{CH}$ manifold, particularly when the UV PROBE is set at 299.105 nm to monitor the $(\nu'_3 + \nu'_5)$ upper state. We therefore postulate that a highly efficient rotationally resolved V−V transfer channel is observable if the UV PROBE wavelength is set at 299.105 nm to excite LIF via the $(\nu'_3 + \nu'_5)$ upper state, whereas that channel is not readily monitored at 296.032 nm via $(\nu'_2 + \nu'_5)$.

We note that collision-induced quasi-continuous background (CIQCB) effects[8,32] appear to be present in virtually all IR−UV DR spectra recorded for the $4\nu_{CH}$ manifold of C_2H_2, as will be further demonstrated elsewhere.[33] This may account entirely for the IR−UV DR signal recorded in the lower trace of Figure 10c, obtained with the UV PROBE at 296.032 nm to excite LIF via the $(\nu'_2 + \nu'_5)$ upper state. Indeed, we have evidence[33] that even apparently discrete IR−UV DR signals (such as those in Figures 2c and 10) contain an underlying contribution from CIQCB effects.[8,32]

The previously reported apparent similarity[8] between IR-scanned IR−UV DR spectra recorded with different UV PROBE transitions is therefore deceptive in this case. There seem to be strong (and surprising) contrasts between IR−UV DR excitation mechanisms that apply to results obtained with the UV PROBE set at ~299.1 nm (as in Figure 2) and at ~296.0 nm (as in Figure 1 of ref 8). Such contrasts have important dynamical implications, indicating other discrete rovibrational states that can be probed more efficiently at 299.105 nm than at 296.032 nm; these rovibrational states are likely to be coupled (either directly or by collisions) to the $(1\,0\,3\,0\,0)^0$ $J = 12$ level, thereby giving rise to the observed "$J = 12$ to $J = 1$" odd-ΔJ RET signals. We have attempted to identify such states that may be coincidentally probed at 299.105 nm along with the $(1\,0\,3\,0\,0)^0$ $J = 1$ level as follows. With the UV PROBE wavelength set at 299.105 nm, IR-scanned IR−UV DR spectra were recorded under effectively collision-free conditions ($P = 200$ mTorr, $t = 10$ ns, $z = 0.033$), using the highest possible instrumental gain to assist detection of particularly weak IR−UV DR parent features arising from rovibrational levels other than those of the $(1\,0\,3\,0\,0)^0$ manifold. This procedure reveals numerous weak IR−UV DR features in the vicinity of the $(\nu_1 + 3\nu_3)$ band, ranging between its P(25) and R(23) IR absorption features. However, no obvious rovibrational assignments can be made by ground-state combination-difference analysis.

Given this uncertainty, we adopt a tentative label, (? ? ? ? ?)$^{?}$ $J = ?$, to denote any unidentified rovibrational state of C_2H_2 that may play a significant mechanistic role in the "$J = 12$ to $J = 1$" odd-ΔJ RET signal. We suppose that at least one such state is IR-dark and (to facilitate intramolecular coupling and rovibrational transfer) close in energy to the $(1\ 0\ 3\ 0\ 0)^0$ $J = 12$ level; its J-value is most likely 11, 12, or 13. Moreover, that IR-dark state (or other states with which it communicates) must be particularly UV-bright when probed at 299.105 nm via the $(\nu'_3 + \nu'_5)$ upper state. The perceived role of such IR-dark, UV-bright rovibrational states has been incorporated, along with that of the CIQCB, in a phenomenological rate-equation model of C_2H_2[8,32,33] A more specific possible mechanism of this form is outlined in section VII below.

It is relevant to recall a significant result from our original report[7] of "$J = 12$ to $J = 1$" odd-ΔJ RET in C_2H_2, using argon (Ar) as a foreign-gas collision partner. Comparing energy-transfer kinetics for C_2H_2/Ar collisions with those for C_2H_2/C_2H_2 self-collisions helps to discriminate between state-to-state *intermolecular* and *intramolecular* rovibrational energy transfer processes. At low vibrational excitation (as in the $V_2 = 1$ manifolds of C_2H_2[48] and C_2D_2[41]), this approach shows that intermolecular V−V transfer between ortho and para nuclear-spin modifications of C_2H_2 or C_2D_2 through self-collisions can yield odd-ΔJ features in DR spectra. An opportunity for such collisional exchange of ortho/para character is absent in C_2H_2/Ar (or C_2D_2/Ar) collisions, where any collision-induced V−V transfer is necessarily intramolecular. We note also previous studies of the effect of C_2H_2/Ar collisions on rovibrational energy transfer in the ν_{CH} region[45,52] and in the $3\nu_{CH}$ region.[38] Likewise, the rovibrational LIF experiments of Halonen et al.[65] yield odd-ΔJ features that are attributable to intermolecular "step-down" V−V transfer between ortho and para modifications of C_2H_2.

In high-overtone vibrational manifolds of C_2H_2 (such as $\nu_{CC} + 3\nu_{CH}$[29−31] or $4\nu_{CH}$[7,8]), appreciable contributions to our IR−UV DR signals from such self-collisional state-to-state intermolecular V−V transfer are considered improbable, because four specific vibrational (CH- and/or CC-stretching) quanta would need to be destroyed in one C_2H_2 molecule and reestablished in the other, while more than 11 000 cm^{-1} of rovibrational energy is exchanged between the state-selected C_2H_2 molecule and its collision partner. It is therefore possible to rule out a relatively trivial possible explanation of apparent odd-ΔJ RET and consequent collision-induced "scrambling" of ortho ($I = 1$, a) and para ($I = 0$, s) nuclear-spin modifications of C_2H_2. This premise[29−31] has been confirmed experimentally[7] by measurements similar to those in Figure 4, with the UV PROBE at 299.105 nm, but comparing IR−UV DR kinetics for neat C_2H_2 with a 1:10 mixture of C_2H_2 in Ar. A remarkable outcome of this kinetic study was that the rate of the "$J = 12$ to $J = 1$" odd-ΔJ RET channel is approximately gas-kinetic, in C_2H_2/Ar collisions as well as in C_2H_2/C_2H_2 collisions. This is consistent with an intramolecular process, in which state-selected C_2H_2 molecules (prepared by the IR PUMP) remain vibrationally excited (and detected by the UV PROBE).

VII. Conclusion: Implications for Rovibrational Dynamics

Sections II, IV, and VI assemble much of the spectroscopic and kinetic evidence from IR−UV DR experiments concerning the $(1\ 0\ 3\ 0\ 0)^0$ $J = 1$ level of C_2H_2 that is monitored by the UV PROBE at 299.105 or 296.032 nm. Associated intramolecular rovibrational energy transfer channels appear to link this level to the $(1\ 0\ 3\ 0\ 0)^0$ $J = 12$ level, which provides a particularly efficient channel for IR PUMP excitation.[7,8] An underlying CIQCB effect[8,32] also offers a ubiquitous means of IR−UV DR excitation, not confined to discretely resonant UV PROBE wavelengths. More information on the latter ($J = 12$ and CIQCB) effects will be presented in a subsequent paper,[33] whereas this paper addresses the former ($J = 1$) processes. Corresponding results for the $(1\ 0\ 3\ 0\ 0)^0$ $J = 0$ level are also presented in section V, but these are ambiguous owing to possible interference from a nearby unassigned IR-dark, UV-bright $J = 10$ rovibrational state (see Figures 8 and 9).

A central issue of this paper concerns the role of low-J rovibrational states of the $4\nu_{CH}$ manifold, notably the $(1\ 0\ 3\ 0\ 0)^0$ $J = 1$ level. We seek to establish the extent to which the IR−UV DR results (Figures 2, 3, 5, and 10) entail UV PROBE excitation from the $(1\ 0\ 3\ 0\ 0)^0$ $J = 1$ level and propose additional mechanisms that (at least tentatively) explain "$J = 12$ to $J = 1$" odd-ΔJ RET processes.

IR-scanned IR−UV DR spectra, as in Figure 2c, and kinetic curves, as in Figures 3 and 10b, show clearly that collisions cause $(1\ 0\ 3\ 0\ 0)^0$ rovibrational levels (prepared by the IR PUMP pulse with $J = 3, 5, 7, ...$) to undergo regular even-ΔJ RET to the $(1\ 0\ 3\ 0\ 0)^0$ $J = 1$ level that is monitored by setting the UV PROBE wavelength at *either* 299.105 *or* 296.032 nm. On the other hand, Figures 2b and 10a show corresponding IR−UV DR parent features that arise instantaneously by direct two-step excitation (IR PUMP then UV PROBE, with no need for collisional mediation). It is less straightforward to understand the apparent odd-ΔJ satellites accompanying regular even-ΔJ RET features, centered around the prominent R(11) and P(13) features of the $(1\ 0\ 3\ 0\ 0)^0$ $J = 12$ level, as in Figures 2c, 3, and 10c. In our original report[7] of IR−UV DR spectra for the $4\nu_{CH}$ manifold, it was proposed that this odd-ΔJ RET arises by an exotic "symmetry-breaking" process. However, odd-ΔJ RET by any intramolecular process in C_2H_2 is considered unlikely if it entails interconversion between the ortho ($I = 1$, a) and para ($I = 0$, s) nuclear-spin modifications of the molecule. A plausible mechanism for the odd-ΔJ RET processes has been advanced,[31] in the parallel context of the $\nu_{CC} + 3\nu_{CH}$ manifold of C_2H_2. It relies on spoiling of the vibrational angular momentum l by Coriolis and rotational l-resonances, together with Stark-type collisional coupling and the possibility that the same set of UV PROBE wavelengths can monitor both components of the l-doublet within the finite optical bandwidth (~0.2 cm^{-1}) of the UV PROBE radiation.

Our rovibrational polyad-model calculations, similar to those in the $\nu_{CC} + 3\nu_{CH}$ manifold,[31] suggest a tentative mechanism for "$J = 12$ to $J = 1$" odd-ΔJ RET in the present context of the $4\nu_{CH}$ manifold.[8] This entails Coriolis coupling at $J = 12$ between the rovibrational manifolds $(1\ 0\ 3\ 0\ 0)^0$ and (? ? ? ? ?)$^{?}$, that is predominantly of Π_u symmetry (i.e., $l = 1$). Each value of J then has e- and f-symmetry levels,[97] amenable to both odd-ΔJ RET and even-ΔJ RET ($e \leftrightarrow f$) within that Π_u manifold. Our polyad-model calculations indicate that this (? ? ? ? ?)$^{?}$ Π_u manifold can be labeled $(0\ 3\ 0\ 10\ 1)^1/(1\ 0\ 2\ 4\ 1)^1$, to reflect its mixed vibrational basis-state parentage, and that it has pseudo-quantum numbers $n_s = 3$, $n_{res} = 20$, and $l = 1$. It is expected to have pronounced IR-dark/UV-bright character, as is the case in our observations. We postulate[8] that "$J = 12$ to $J = 1$" odd-ΔJ RET is mediated by Coriolis coupling ($e \leftrightarrow e$) between the IR-pumped $(1\ 0\ 3\ 0\ 0)^0$ and $(0\ 3\ 0\ 10\ 1)/(1\ 0\ 2\ 4\ 1)^1$ $J = 12$ levels. This, we propose, is followed by $\Delta J = -11$ RET ($e \leftrightarrow f$) in the Π_u manifold to the IR-dark/UV-bright $(0\ 3\ 0\ 10\ 1)/(1\ 0\ 2\ 4\ 1)^1$ $J = 1$ level, from which LIF can be excited

(we suppose) at the same UV PROBE wavelength (299.105 nm) as LIF from the IR-bright $(1\ 0\ 3\ 0\ 0)^0$ $J = 1$ level.

It is ironic that the anomalously large Stark effect[66] of the low-J portion of the $(1\ 0\ 3\ 0\ 0)^0$ manifold of C_2H_2 initially stimulated interest in IR−UV DR studies of that region[7] but is apparently no longer needed in the mechanism that has gained favor[8] over the original (now discredited) *a*/*s*-symmetry-breaking mechanism.[7] Another irony is the fact that collision-induced Stark-type *g*/*u* mixing remains essential in mechanisms applied to odd-ΔJ RET in the $\nu_{CC} + 3\nu_{CH}$ manifold of C_2H_2,[31,68] but not in those for the $4\nu_{CH}$ manifold. Such collision-induced Stark mixing may still be needed to explain other aspects such as the ubiquitous (but poorly understood) CIQCB effects.[8,32] Key issues such as these will be addressed in subsequent papers.[33] In the meantime, the present "foundation studies at low *J*" (to which the subtitle of this paper alludes) have demonstrated the attention to detail that is essential in IR−UV DR experiments that seek unambiguous characterization of the rovibrational dynamics of a small but not-so-simple polyatomic molecule such as C_2H_2.

Acknowledgment. Financial support from the Australian Research Council (ARC) is gratefully acknowledged, including the award of an ARC Postdoctoral Fellowship to A.P.M.

References and Notes

(1) Oka, T. *Adv. At. Mol. Phys.* **1973**, *9*, 127.
(2) Yardley, J. T. *Introduction to Molecular Energy Transfer*; Academic Press: New York, 1980.
(3) Flynn, G. W.; Parmenter, C. S.; Wodtke, A. M. *J. Phys. Chem.* **1996**, *100*, 12817.
(4) Nesbitt, D. J.; Field, R. W. *J. Phys. Chem.* **1996**, *100*, 12735.
(5) Bacic, Z.; Miller, R. E. *J. Phys. Chem.* **1996**, *100*, 12945.
(6) Herman, M.; Liévin, J.; Vander Auwera, J.; Campargue, A. *Adv. Chem. Phys.* **1999**, *108*, 1.
(7) Payne, M. A.; Milce, A. P.; Frost, M. J.; Orr, B. J. *Chem. Phys. Lett.* **1997**, *265*, 244.
(8) Payne, M. A.; Milce, A. P.; Frost, M. J.; Orr, B. J. *Chem. Phys. Lett.* **2000**, *324*, 48.
(9) Smith, B. C.; Winn, J. S. *J. Chem. Phys.* **1991**, *94*, 4120.
(10) Herman, M.; Abbouti Temsamani, M.; Lemaitre, D.; Vander Auwera, J. *Chem. Phys. Lett.* **1991**, *185*, 220.
(11) Zhan, X.; Halonen, L. *J. Mol. Spectrosc.* **1993**, *160*, 464.
(12) Herregodts, F.; Hurtmans, D.; Vander Auwera, J.; Herman, M. *J. Chem. Phys.* **1999**, *111*, 7954.
(13) Herregodts, F.; Hepp, M.; Hurtmans, D.; Vander Auwera, J.; Herman, M. *J. Chem. Phys.* **1999**, *111*, 7961.
(14) Herregodts, F.; Hurtmans, D.; Vander Auwera, J.; Herman, M. *Chem. Phys. Lett.* **2000**, *316*, 460.
(15) Hurtmans, D.; Kassi, S.; Depiesse, C.; Herman, M. *Mol. Phys.* **2002**, *100*, 3507.
(16) El Idrissi, M. I.; Liévin, J.; Campargue, A.; Herman, M. *J. Chem. Phys.* **1999**, *110*, 2074.
(17) Halonen, L.; Child, M. S.; Carter, S. *Mol. Phys.* **1982**, *47*, 1097.
(18) Child, M. S.; Halonen, L. *Adv. Chem. Phys.* **1984**, *57*, 1.
(19) Kellman, M.; Chen, G. *J. Chem. Phys.* **1991**, *95*, 8671.
(20) Abboutti Temsamani, M.; Herman, M.; Solina, S. A. B.; O'Brien, J. P.; Field, R. W. *J. Chem. Phys.* **1996**, *105*, 11357.
(21) Khilinski, B. I.; El Idrissi, M. I.; Herman, M. *J. Chem. Phys.* **2000**, *113*, 7885.
(22) El Idrissi, M. I.; Khilinski, B. I.; Gaspard, P.; Herman, M. *Mol. Phys.* **2003**, *101*, 595.
(23) Solina, S. A. B.; O'Brien, J. P.; Field, R. W.; Polik, W. F. *J. Phys. Chem.* **1996**, *100*, 7797.
(24) O'Brien, J. P.; Jacobson, M. P.; Sokol, J. J.; Coy, S. L.; Field, R. W. *J. Chem. Phys.* **1998**, *108*, 7100.
(25) Jacobson, M. P.; O'Brien, J. P.; Silbey, R. J.; Field, R. W. *J. Chem. Phys.* **1998**, *109*, 121.
(26) Jacobson, M. P.; O'Brien, J. P.; Field, R. W. *J. Chem. Phys.* **1998**, *109*, 3831.
(27) Hoshina, K.; Iwasaki, A.; Yamanouchi, K.; Jacobson, M. P.; Field, R. W. *J. Chem. Phys.* **2001**, *114*, 7424.
(28) Milce, A. P.; Barth, H.-D.; Orr, B. J. *J. Chem. Phys.* **1994**, *100*, 2398.
(29) Milce, A. P.; Orr, B. J. *J. Chem. Phys.* **1996**, *104*, 6423.
(30) Milce, A. P.; Orr, B. J. *J. Chem. Phys.* **1997**, *106*, 3592.
(31) Milce, A. P.; Orr, B. J. *J. Chem. Phys.* **2000**, *112*, 9319.
(32) Payne, M. A. Ph.D. Thesis, Macquarie University, Sydney, Australia, 1999.
(33) Payne, M. A.; Milce, A. P.; Frost, M. J.; Orr, B. J. Unpublished results.
(34) Carrasquillo M., E.; Utz, A. L.; Crim, F. F. *J. Chem. Phys.* **1988**, *88*, 5976.
(35) Utz, A. L.; Tobiason, J. D.; Carrasquillo, M. E.; Fritz, M. D.; Crim, F. F. *J. Chem. Phys.* **1992**, *97*, 389.
(36) Tobiason, J. D.; Utz, A. L.; Crim, F. F. *J. Chem. Phys.* **1992**, *97*, 7437.
(37) Tobiason, J. D.; Utz, A. L.; Crim, F. F. *J. Chem. Phys.* **1994**, *101*, 1108.
(38) Tobiason, J. D.; Fritz, M. D.; Crim, F. F. *J. Chem. Phys.* **1994**, *101*, 9642.
(39) Utz, A. L.; Carrasquillo, M. E.; Tobiason, J. D.; Crim, F. F. *Chem. Phys.* **1995**, *190*, 311.
(40) Chadwick, B. L.; King, D. A.; Berzins, L.; Orr, B. J. *J. Chem. Phys.* **1989**, *91*, 7994.
(41) Chadwick, B. L.; Orr, B. J. *J. Chem. Phys.* **1991**, *95*, 5476.
(42) Dopheide, R.; Gao, W. B.; Zacharias, H. *Chem. Phys. Lett.* **1991**, *182*, 21.
(43) Chadwick, B. L.; Orr, B. J. *J. Chem. Phys.* **1992**, *97*, 3007.
(44) Frost, M. J.; Smith, I. W. M. *Chem. Phys. Lett.* **1992**, *191*, 574.
(45) Frost, M. J. *J. Chem. Phys.* **1993**, *98*, 8572.
(46) Dopheide, R.; Zacharias, H. *J. Chem. Phys.* **1993**, *99*, 4864.
(47) Chadwick, B. L.; Milce, A. P.; Orr, B. J. *Chem. Phys.* **1993**, *175*, 113.
(48) Chadwick, B. L.; Milce, A. P.; Orr, B. J. *Can. J. Phys.* **1994**, *72*, 939.
(49) Frost, M. J.; Smith, I. W. M. *J. Phys. Chem.* **1995**, *99*, 1094.
(50) Henton, S.; Islam, M.; Smith, I. W. M. *Chem. Phys. Lett.* **1998**, *291*, 223.
(51) Henton, S.; Islam, M.; Smith, I. W. M. *J. Chem. Soc., Faraday Trans.* **1998**, *94*, 3207.
(52) Henton, S.; Islam, M.; Gatenby, S.; Smith, I. W. M. *J. Chem. Soc., Faraday Trans.* **1998**, *94*, 3219.
(53) Rudert, A. M.; Martin, J.; Gao, W.-B.; Halpern, J. B.; Zacharias, H. *J. Chem. Phys.* **1999**, *111*, 9549.
(54) Rudert, A. M.; Martin, J.; Gao, W.-B.; Zacharias, H.; Halpern, J. B. *J. Chem. Phys.* **2000**, *112*, 9749.
(55) Orr, B. J.; Smith, I. W. M. *J. Phys. Chem.* **1987**, *91*, 6106.
(56) Orr, B. J. *Chem. Phys.* **1995**, *190*, 261.
(57) Orr, B. J. In *Advances in Chemical Kinetics and Dynamics−Vibrational Energy Transfer Involving Large and Small Molecules*; Barker, J. R., Ed.; JAI Press: Greenwich, CN., 1995; Vol. 2A, p 21.
(58) Jonas, D. M.; Solina, S. A. B.; Rajaram, B.; Silbey, R. J.; Field, R. W.; Yamanouchi, K.; Tsuchiya, S. *J. Chem. Phys.* **1993**, *99*, 7350.
(59) Moss, D. B.; Duan, Z.; Jacobson, M. P.; O'Brien, J. P.; Field, R. W. *J. Mol. Spectrosc.* **2000**, *199*, 265.
(60) Silva, M.; Jongma, R.; Field, R. W.; Wodtke, A. M. *Annu. Rev. Phys. Chem.* **2001**, *52*, 811.
(61) Solina, S. A. B.; O'Brien, J. P.; Field, R. W.; Polik, W. F. *Ber. Bunsen-Ges. Phys. Chem.* **1995**, *99*, 555.
(62) Silva, M. L.; Jacobson, M. P.; Duan, Z.; Field, R. W. *J. Chem. Phys.* **2002**, *116*, 7939.
(63) Jungner, P.; Halonen, L. *J. Chem. Phys.* **1997**, *107*, 1424.
(64) Saarinen, M.; Permogorov, D.; Halonen, L. *J. Chem. Phys.* **1999**, *110*, 1424.
(65) Metsala, M.; Yang, S.; Vaittinen, O.; Halonen, L. *J. Chem. Phys.* **2002**, *117*, 8686.
(66) Barnes, J. A.; Gough, T. E.; Stoer, M. *Chem. Phys. Lett.* **1995**, *237*, 437.
(67) Barnes, J. A.; Gough, T. E.; Stoer, M. *Rev. Sci. Instrum.* **1999**, *70*, 3515.
(68) Barnes, J. A.; Gough, T. E.; Stoer, M. *J. Chem. Phys.* **2001**, *114*, 4490.
(69) Mizoguchi, M.; Yamakita, N.; Tsuchiya, S.; Iwasaki, A.; Hoshina, K.; Yamanouchi, K. *J. Phys. Chem. A* **2000**, *104*, 10212.
(70) Arusi-Parpar, T.; Schmid, R. P.; Ganot, Y.; Bar, I.; Rosenwaks, S. *Chem. Phys. Lett.* **1998**, *287*, 347.
(71) Schmid, R. P.; Ganot, Y.; Bar, I.; Rosenwaks, S. *J. Chem. Phys.* **1998**, *109*, 8959.
(72) Sheng, X.; Ganot, Y.; Rosenwaks, S.; Bar, I. *J. Chem. Phys.* **2002**, *117*, 6511.
(73) Jacobson, M. P.; Field, R. W. *J. Phys. Chem. A* **2000**, *104*, 3073.
(74) Schork, R.; Köppel, J. M. *J. Chem. Phys.* **2001**, *115*, 7907.
(75) Zou, S.; Bowman, J. M. *J. Chem. Phys.* **2002**, *116*, 6667.
(76) Loh, Z.-H.; Field, R. W. *J. Chem. Phys.* **2003**, *118*, 4037.
(77) Coveleskie, R. A.; Dolson, D. A.; Parmenter, C. S. *J. Phys. Chem.* **1985**, *89*, 645/655.
(78) Holtzclaw, K. W.; Parmenter, C. S. *J. Chem. Phys.* **1986**, *84*, 1099.

(79) Dolson, D. A.; Holtzclaw, K. W.; Moss, D. B.; Parmenter, C. S. *J. Chem. Phys.* **1986**, *84*, 1119.
(80) Oudejans, I.; Moore, D. T.; Miller, R. E. *J. Chem. Phys.* **1999**, *110*, 209.
(81) Oudejans, I.; Miller, R. E. *J. Phys. Chem. A* **1999**, *103*, 4791.
(82) Oudejans, I.; Miller, R. E. *Annu. Rev. Phys. Chem.* **2001**, *52*, 607.
(83) Butz, K. W.; Du, H.; Krajnovich, D. J.; Parmenter, C. S. *J. Chem. Phys.* **1988**, *89*, 4680.
(84) Gilbert, B. D.; Parmenter, C. S.; Krajnovich, D. J. *J. Phys. Chem.* **1994**, *98*, 7116.
(85) Gilbert, B. D.; Parmenter, C. S.; Krajnovich, D. J. *J. Chem. Phys.* **1994**, *101*, 7423.
(86) Gilbert, B. D.; Parmenter, C. S. *J. Chem. Phys.* **1994**, *101*, 7440.
(87) Clegg, S. M.; Burrill, A. B.; Parmenter, C. S. *J. Phys. Chem. A* **1998**, *102*, 8477.
(88) Clegg, S. M.; Parmenter, C. S. *J. Phys. Chem. A* **2000**, *104*, 10265.
(89) Parmenter, C. S.; Clegg, S. M.; Krajnovich, D. J.; Lu, S.-P. *Proc. Natl. Acad. Sci. U.S.A.* **1997**, *94*, 8387.
(90) Schmid, G. M.; Coy, S. L.; Field, R. W.; Silbey, R. J. *J. Chem. Phys.* **1994**, *101*, 869.
(91) Baxter, G. W.; Payne, M. A.; Austin, B. D. W.; Halloway, C. A.; Haub, J. G.; He, Y.; Milce, A. P.; Nibler, J. W.; Orr, B. J. *Appl. Phys. B* **2000**, *71*, 651.
(92) Tobiason, J. D. Ph.D. Thesis, University of Wisconsin—Madison, Madison, WI, 1992.
(93) Hougen, J T.; Watson, J. K. G. *Can. J. Phys.* **1965**, *43*, 298.
(94) Huet, T. R.; Godefroid, M.; Herman, M. *J. Mol. Spectrosc.* **1990**, *144*, 32.
(95) Utz, A. L.; Tobiason, J. D.; Carrasquillo M., E.; Sanders, L. J.; Crim, F. F. *J. Chem. Phys.* **1993**, *98*, 2742.
(96) Tobiason, J. D.; Utz, A. L.; Crim, F. F. *J. Chem. Phys.* **1993**, *99*, 928.
(97) Brown, J. M.; Hougen, J. T.; Huber, K.-P.; Johns, J. W. C.; Kopp, I.; Lefebvre-Brion, H.; Merer, A. J.; Ramsay, D. A.; Rostas, J.; Zare, R. N. *J. Mol. Spectrosc.* **1975**, *55*, 500.